

Skeleton coupling: a novel interlayer mapping of community evolution in temporal networks

Bengier Ülgen Kilic^{1,*} and Sarah Feldt Muldoon^{1,2,3,†}

¹*Department of Mathematics, University at Buffalo, SUNY, New York, USA*

²*CDSE program, University at Buffalo, SUNY, New York, USA*

³*Neuroscience program, University at Buffalo, SUNY, New York, USA*

(Dated: January 27, 2023)

Abstract

Dynamic community detection (DCD) in temporal networks is a complicated task that involves the selection of an algorithm and its associated parameters. How to choose the most appropriate algorithm generally depends on the type of network being analyzed and the specific properties of the data that define the network. In functional temporal networks derived from neuronal spike train data, communities are expected to be transient, and it is common for the network to contain multiple singleton communities. Here, we compare the performance of different DCD algorithms on functional temporal networks built from synthetic neuronal time series data with known community structure. We find that, for these networks, DCD algorithms that utilize interlayer links to perform community carryover between layers outperform other methods. However, we also observe that algorithm performance is highly dependent on the topology of interlayer links, especially in the presence of singleton and transient communities. We therefore define a novel method for defining interlayer links in temporal networks called skeleton coupling that is specifically designed to enhance the linkage of communities in the network throughout time based on the topological properties of the community history. We show that integrating skeleton coupling with current DCD methods improves algorithm performance in synthetic data with planted singleton and transient communities. The use of skeleton coupling to perform DCD will therefore allow for more accurate and interpretable results of community evolution in real-world neuronal data or in other systems with transient structure and singleton communities.

* bengieru@buffalo.edu

† smuldoon@buffalo.edu

I. INTRODUCTION

Complex systems are often composed of elements whose dynamics and interactions can change over time. Such temporal events might describe human communication [1], proximity [2–4], trade and transportation [5, 6], citation and collaboration [7, 8], or biological [9, 10] and neuronal interactions [11, 12]. Modeling these systems as temporal networks [13, 14] can be useful, as network nodes and edges can capture temporal properties of the data. This is particularly relevant for systems with nodes whose dynamics can be represented using time series data.

Neuronal systems are a prime example of a dynamic system that can be modeled as a temporal network. For example, spike train data describes the simultaneous firing patterns of neurons over time. Thus, one can build a network whose nodes are neurons and whose edges represent statistical relationships (such as synchronization or some other similarity measure) between the firing patterns of neurons. In order to capture the fact that interactions between pairs of neurons will change over time, a common way of building a temporal network with this data is to create sequential snapshots of the network over time that describe the dynamic evolution of the data. To do this, one can split the time series into smaller time series, construct chronologically ordered set of network states, and try to characterize the intrinsic patterns of connectivity across those individual snapshots (Fig. 1A).

One aspect of temporal networks that is often of interest to study is the dynamic properties of communities within the network over time. In our example of neuronal firing, communities could represent synchronized groups of neurons, and we could ask how the membership of such groups changes over time. Multiple dynamic community detection (DCD) algorithms have been developed that extend static community detection to temporal networks, where now communities can exist (and be created/die) across time [15]. However, similar to the case of static networks, each DCD algorithm is based on a slightly different definition of how communities are detected within the network. Further, DCD algorithms must also include a definition of how to properly carry-over or assign community labels across snapshots (layers of the network). As a result, DCD algorithms in the literature vary greatly depending on their treatment of the snapshots and their temporal dependence [16]. Some algorithms treat individual snapshots separately, others might iterate over the snapshots in chronological order, and some might use interlayer edges to link the snapshots over time into a temporally connected network.

Here, we focus on five commonly used DCD algorithms that span the different ways of defining dynamic communities: Multilayer modularity maximization (MMM) [17], Infomap [18, 19], Dynamic stochastic block model (DSBM) [20, 21], Dynamic plex propagation method (DPPM) [22], and Tensor Factorization [23]. MMM and DSBM define a community as a densely connected cluster of nodes with respect to a null model, whereas Infomap defines a community as a group of nodes in which information flows quickly and efficiently. DPPM utilizes a definition in which communities are groups of subsets (plexes) of fully connected subgraphs (cliques) that have maximal overlap. Finally, Tensor Factorization takes an approach from linear algebra and defines the communities as the bases of a vector space generating the underlying network.

This variance in the definitions of a dynamic community forces these algorithms to make specific assumptions about how to temporally carry-over community labels across snapshots (layers) (Fig. 1B). Algorithms like MMM and Infomap operate on the idea that temporal carry-over is performed through the structural multilayer network topology; in this case ‘interlayer edges’ are defined that link nodes across layers, such that communities can naturally exist across time. However, the other three algorithms use ‘fixed rules’ to define temporal carry-over that ignore data-specific differences. DSBM uses a fixed generative model for the temporal network in which communities are created and transferred across time via a Bayesian method. DPPM uses a fixed algorithm in which plexes in static layers are carried over across time if they intersect sufficiently between snapshots. Finally, Tensor Factorization utilizes a fixed factorization technique (PARAFAC) that splits the 3-way tensor into simpler matrices in which the time component of the factorization corresponds to the temporal carry-over.

Importantly, because of the different ways in which each algorithm defines a community, both statically and dynamically, different algorithms will emphasize different features of the data and therefore will detect different patterns of dynamic communities. It is therefore essential to have an understanding of how each algorithm detects the specific features of the data and incorporates this information into the detected communities. This is especially relevant in order to interpret any results when these algorithms are applied to experimental data sets where the underlying ground truth is not known. Motivated by our example from neuroscience, here we are especially interested in how various DCD algorithms perform to detect data with a high presence of singleton communities (independently firing neurons) and transient communities (cell assemblies that change over time with the state of the brain). We therefore simulate spike train data with known community structure and test the performance of DCD algorithms on this data.

As expected, we find that different algorithms detect different patterns of dynamic community structure for the same data set. Algorithms that incorporate interlayer edges to link snapshots over time perform better at detecting singleton and transient communities in our simulated data, but all algorithms struggle to correctly perform temporal carry-over of community labels. We find that the topology of how interlayer links are defined in these temporal networks can greatly influence the performance of the algorithm. The most common method of interlayer coupling, called diagonal coupling, in which network nodes are linked to themselves in sequential layers, performs poorly at properly assigning the carry-over of community labels in our data. However, we find that by utilizing information about the *intralayer* topology of each individual layer in the network to couple the layers, one can improve algorithm performance.

Using methods from topological data analysis (TDA), a field in the intersection of data science and algebraic topology in

mathematics [24–27], we define a novel interlayer coupling method called skeleton coupling that defines interlayer edges based on the community information within the static layers of temporal networks. Skeleton coupling takes the temporal neighborhood history and community assignment of a vertex (in the adjacent past state) into account such that DCD algorithms robustly and correctly capture the temporal carry-over of both singleton communities and larger assemblies. We compare our results for skeleton coupling with previously proposed mechanisms of interlayer coupling and show that skeleton coupling outperforms other methods on data with a high prevalence of singleton and transient communities.

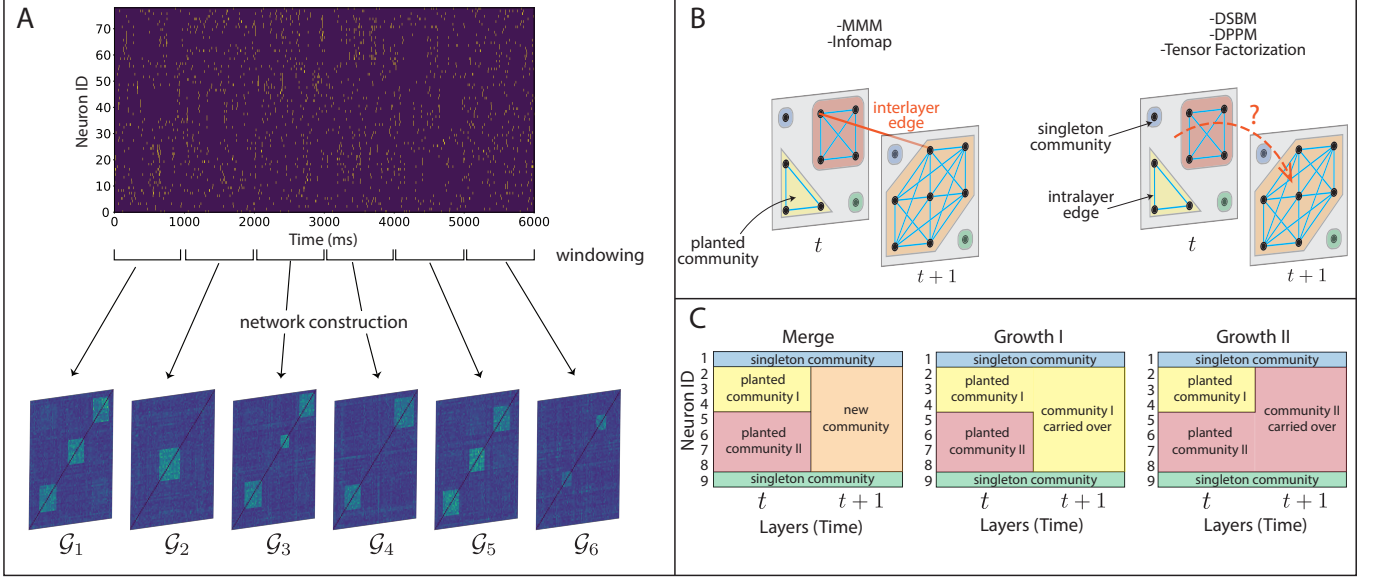


FIG. 1. **From time-series to dynamic community analysis** **A.** A synthetic time-series from $N = 78$ neurons generated via homogeneous Poisson process which contains planted communities undergoing community events at every $\tau = 1000$ ms. The data is divided into 1000ms windows and six functional network snapshots representing the co-activity of neurons are constructed by calculating the maximum cross-correlation between pairs of spike trains. **B.** A two-snapshot dynamic network in which temporal carryovers are performed via either *interlayer edges* by MMM and Infomap (left) or by some *fixed rule* by DSBM, DPPM and Tensor Factorization (right). **C.** Three different scenarios for the community events taking place in part B. On the left, two planted communities in t ‘merge’ so that the resulting community in $t + 1$ has a new community label. In the middle, planted community I ‘grows’ by joining with planted community II, and the resulting community has the same label as I. On the right, planted community II ‘grows’ by joining with planted community I, and the resulting community gets the label II. Different DCD algorithms handle these types of carryovers differently.

II. SIMULATION OF NEURONAL DATA

As previously mentioned, this work is motivated by applications for studying temporal functional networks built from firing patterns of individual neurons. However, because in such data the ground truth of community evolution cannot be known, here we apply our analysis to synthetic data. Although previous work studying community evolution has designed benchmark networks for testing community detection in evolving networks [28–31], the links in these networks represent structural (as opposed to functional) connections between nodes. As such, these benchmark models do not generally contain singleton communities or highly transient communities as commonly seen in functional networks based on correlation data [32–34]. We therefore designed a set of functional benchmark networks built from correlations between simulated neuronal spike trains.

In our numerical experiments, we study two different types of community events expected to be present in dynamic functional networks: monotonic and non-monotonic events. Monotonic events correspond to the scenarios where a graph progressively evolves over time such that communities in one layer are nested into the communities in an adjacent layer. Such events include community expansion, shrinkage, or continuation. Non-monotonic events represent the scenarios in which communities in adjacent layer can partially overlap (as in Fig. 1A), but these communities do not necessarily contain each other. Examples of non-monotonic events include community merging, splitting, death, and birth. In each of these scenarios, it is necessary to properly determine how the community labels should evolve over time, as depending on the properties of the data (such as neuronal firing pattern or rate), one might want to either define a new community, or carryover a previous label (see Fig. 1(B-C)).

Here, we focus on examples of a monotonic event (an expanding community) and a non-monotonic event (multiple transient communities). Community structure is modeled using simulated neuronal spiking activity with built-in correlations between firing patterns of individual neurons within a given community. In addition, the community structure (correlated firing of

neurons) is allowed to dynamically evolve through a series of community events. Importantly, in this data, multiple neurons have independent firing patterns, such that many singleton communities are present in the data.

In order to map this data to a temporal network, the time series is first divided into multiple windows, each representing a layer of the network. Functional network structure in each layer is obtained by computing the absolute value of the pairwise maximum cross-correlation between firing patterns of neurons over the window. Because the use of cross-correlations to define functional network connections results in a fully connected network with many small edge weight values that likely represent noise in the data, for each data set, we create a set of temporal networks in which a threshold is used to eliminate connections with edge weights below the threshold value. In the following section, all results are presented across a range of threshold values (shown along the x-axis in the parameter space maps of Figs. 2, 5, and 6). Please see Methods for further details of synthetic data generation and network creation.

III. COMPARISON OF DCD ALGORITHM PERFORMANCE

We compare the performance of 5 different DCD algorithms (MMM [17], Infomap [35], DSBM [20], DPPM [22] and Tensor Factorization [23]) on two different community evolution scenarios as described above (expanding and transient communities). We include a range of algorithm specific hyperparameters (resolution parameter γ , multilayer relax rate ρ , degree correction Δ , k-plex dimension k , and input tensor rank η , respectively) as the y-axes of parameter space maps for these 5 algorithms.

In the left panels of Fig. 2A and Fig. 2B, we display the ground truth of the community evolution of planted dynamic communities. We then plot the parameter space describing the performance of the algorithm as a function of the normalized mutual information (NMI) [36, 37] with respect to the ground truth (See Methods Section ‘Evaluating partition quality’). In these plots, the parameter values representing the optimal performance of each algorithm are indicated by the region bounded by the green rectangle (See Methods Section ‘Optimal regions’). An example of the community evolution in this optimal regime is shown below the parameter space plot.

In Fig. 2(A), we present the performance of the 5 DCD algorithms to detect the community evolution of an expanding community event. Neurons first exist as singleton communities (firing patterns are uncorrelated with others) and join a growing correlated community as time advances (series of monotonic events). As seen in the NMI parameter landscapes, each algorithm varies in its ability to correctly detect this pattern of community evolution. Example community evolution plots and respective parameters are shown for the optimal algorithm performance below these plots. It can be observed that the MMM and Infomap algorithms perform the best at detecting singleton communities and performing temporal carryover; these algorithms also produce the highest NMI values (darker shade of red) over a wider range of parameters. Still, MMM fails to properly detect the expanding community, whereas Infomap partially detects this growing community, albeit with some noise. DSBM and DPPM, on the other hand, yield relatively low NMI and result in the detection of 2 total communities, as they do not properly distinguish the singleton communities and instead lump all uncorrelated neurons into a single community. Tensor Factorization performs somewhere in-between these extremes and detects most of the communities in individual layers separately, failing to properly perform temporal carryover.

We next compare the performance of the algorithms on data containing transient and singleton communities (non-monotonic events; Fig. 2B). Again, we observe that MMM and Infomap perform the best as measured by the NMI, but the optimal community partitions shows that they are detecting rather different patterns of community evolution. Both algorithms are able to detect singleton communities and perform temporal carryover on the singleton communities. MMM additionally, detects some of the transient larger communities, but fails to perform temporal carryover between layers for these transient communities. Tensor Factorization can also detect the transient communities in addition to singleton communities but completely fails at performing temporal carryover of community layers. Once again, DSBM and DPPM only detect two communities which does not reflect the planted structure and is apparent in their low NMI values.

It is notable that in each of the scenarios studied, the DSBM and DPPM algorithms were unable to detect the presence of singleton communities in the data. Further, Tensor Factorization consistently failed to perform temporal carryover of detected communities. While MMM and Infomap did not always perform the temporal carryover correctly, they were able to identify singleton communities, and importantly, these algorithms rely on interlayer edges to link layers across time. In the data presented above, for the MMM and Infomap algorithms, the standard technique of diagonal coupling was used, as this is the most commonly employed method of coupling. However, this is another parameter that can be tweaked when using these algorithms, and for the remainder of this paper, we will focus on the use of different methods of interlayer coupling to further improve community detection in the MMM and Infomap algorithms.

IV. TRADITIONAL INTERLAYER COUPLING

When employing the MMM and Infomap algorithms in a temporal network, the network must be constructed by using interlayer edges that describe how nodes are linked across layers (and therefore across time). Here we review some standard

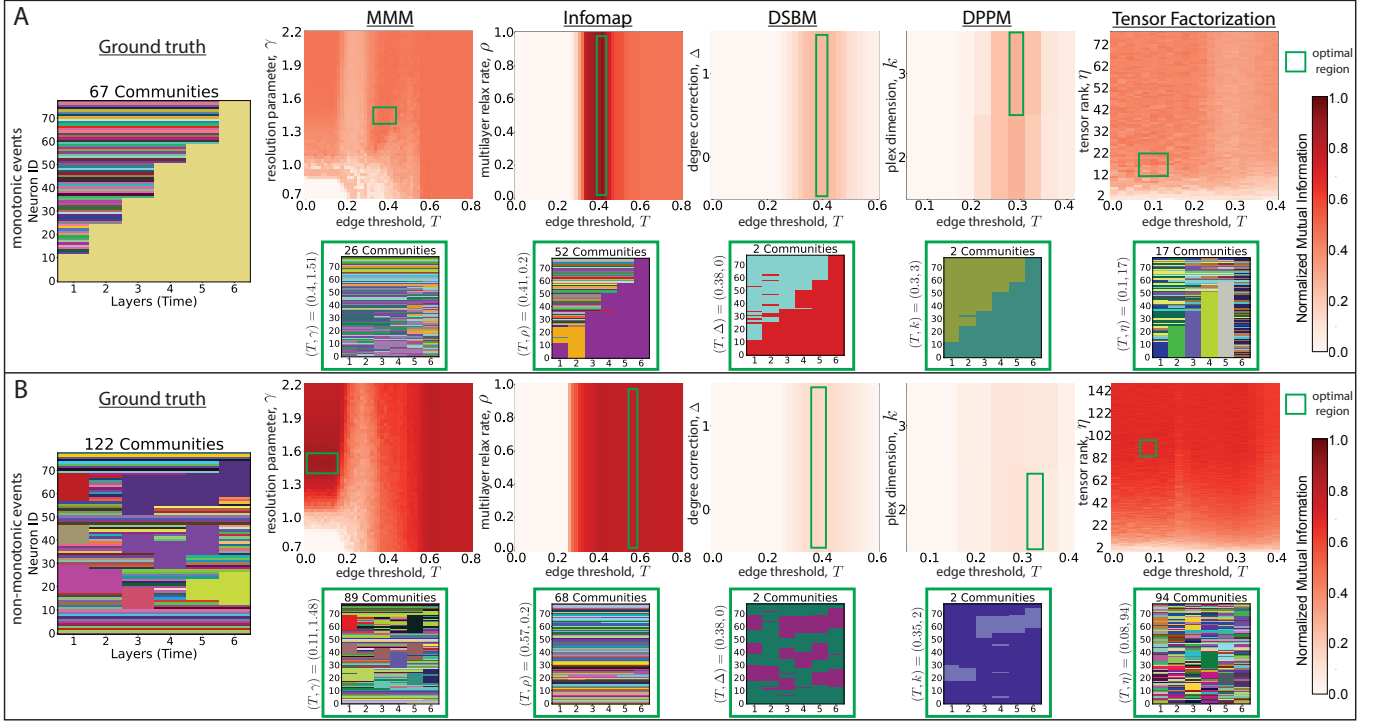


FIG. 2. Comparing DCD algorithms on simulated time series. A comparison of algorithm performance across parameter spaces and *example partitions* for the optimal regions of five different DCD algorithms: MMM, Infomap, DSBM, DPPM and Tensor Factorization. Algorithm performance is explored as a function of the edge threshold, T , and an algorithm-specific parameter (resolution parameter γ , multilayer relax rate ρ , degree correction Δ , k -plex size k and tensor rank η , respectively) by plotting the normalized mutual information (NMI) between the ‘ground truth’ community labels (left panel) and predicted labels. The optimal region is defined as the parameter values (T, \cdot) in which NMI is maximized, and an *example partition* from this region is shown under each parameter grid. Partition plots represent the community evolution across six snapshots (network layers) and the colors indicate the community label of each neuron at each point in time. **A.** Dynamics of $N = 78$ spiking neurons are simulated such that a large community keeps expanding by merging with singleton communities at every layer (monotonic event). There are 67 community labels in total during the ground truth community evolution. **B.** Dynamics of $N = 78$ spiking neurons are simulated such that synchronized groups of neurons appear and disappear over time i.e. *transient communities*, and neurons that are not part of any community are assigned a unique community label (indicated by colors) that is temporally carried over unless a neuron undergoes a community event. A total of 122 community labels are produced during this event as shown in the ground truth partition plot.

and recently proposed methods for defining interlayer links in temporal networks. Let $\mathbb{T} = (V, E)$ be a node-aligned temporal network with snapshot representation $\mathbb{T} = \{G_1, G_2, \dots, G_{t_{max}}\}$. We’ll denote the node σ_α in the layer G_t by σ_α^t and an undirected edge from σ_α^t to another node σ_β^s by $(\sigma_\alpha^t, \sigma_\beta^s)$.

A. Diagonal coupling

The most common way of constructing interlayer edges is to use diagonal coupling. In this case, each node of the network is coupled with its temporal counterpart in a regular fashion as in Fig.3A. Thus, there exists an interlayer edge $(\sigma_\alpha^t, \sigma_\alpha^{t+1})$ for all α and for all $t \in \{1, 2, \dots, t_{max} - 1\}$ with edge weight ω , where ω is constant across all edges, but its value must be specified by the user. Here, ω can be thought of as a self-identity link that preserves the identity of the node throughout time. We will refer to this method of coupling as *uniform diagonal coupling*.

While this method of coupling will allow for a node to maintain its identity throughout the network, it does not capture the fact that in many networks, the nodes represent dynamic entities whose properties change throughout time. A question one may ask is if changing the values of the interlayer edge weights (i.e., allowing for ω to vary across nodes and layers) would make a difference in the detection of dynamic communities. Each diagonal interlayer edge is a link from a node to its future or past self, so in this sense, these links indicate the strength of temporal self-similarity of nodes. In our simulated data, the nodes are in fact neurons whose firing rates and patterns can evolve, thus a nodes self-similarity over time is not necessarily constant. Previous work [38] has described a method that allows for the value of ω to change based on the level of nodal self-similarity. The greater the change in the self-similarity of a node is between snapshots (e.g. the firing rate of the neuron), the weaker the nodes interlayer

edge weight is between the corresponding temporal layers. We refer to this method as *diagonal coupling with local updates* and, mathematically, we assign an interlayer edge between σ_α^t and σ_α^{t+1} for all α and for all $t \in \{1, 2, \dots, t_{max} - 1\}$ with edge weight ω_α^t depending on the spike rate change in node σ_α from G_t to G_{t+1} . See the Methods Section ‘Interlayer coupling’ for details.

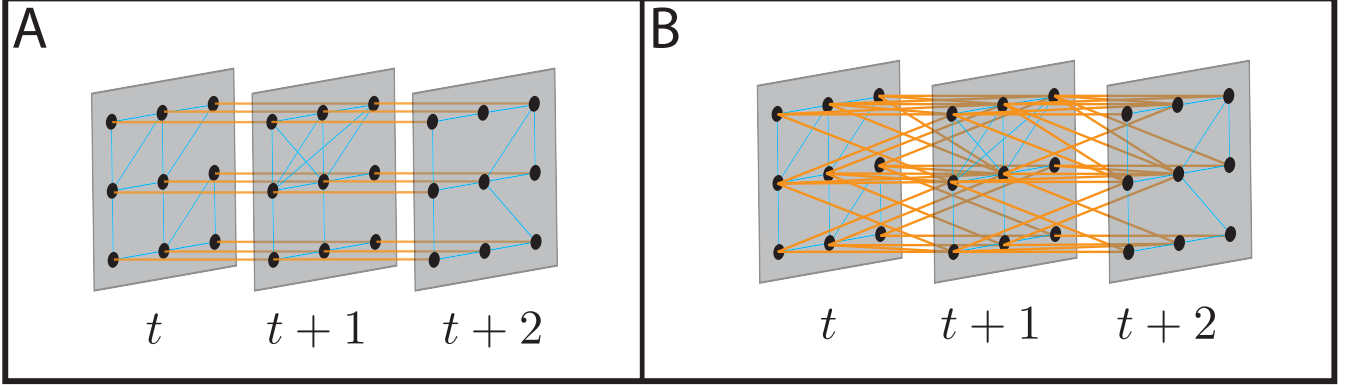


FIG. 3. **Types of interlayer coupling heuristics.** **A.** Diagonal coupling. Nodes are only allowed to be connected to their past and future self with a uniform edge weight (uniform coupling). A modification to this (local updates) can be done by dynamically altering the edge weights based on a self-similarity metric of the node from time t to $t + 1$. **B.** Non-diagonal coupling. Interlayer coupling can exist between any pair of nodes. In the example, we illustrate neighborhood coupling which connects neighborhoods of every node with the adjacent layer.

B. Non-diagonal coupling

While diagonal coupling only allows for a link between a node and itself across layers of the network, it is also completely reasonable to relax this restriction and allow links between some or all pairs of nodes, which introduces a new dimension of complexity and increases the size of the parameter space enormously. While there are multiple ways that one could perform a non-diagonal coupling scheme, here we highlight one previously proposed method called *neighborhood coupling* [39], that connects a maximal neighborhood around every node with the adjacent layers (Fig.3B). Mathematically, we assign interlayer edges of constant weight ω from σ_α^t to a set $\{\sigma_\beta^{t+1}\}_{\beta \in N_\alpha^t}$ such that σ_β is in the maximal neighborhood of σ_α^t in terms of edge weight (strongly connected neighbors of σ_α in G_t) where $N_\alpha^t = \{\sigma_\beta^t | (\sigma_\beta^t, \sigma_\alpha^t) \in E_t\}$. See the Methods Section ‘Interlayer coupling’ for details. This method of coupling is based on the assumption that the topology of the network in its previous state affects how the network evolves. Note that this method also results in a more dense coupling than that of diagonal coupling as seen in Fig. 3B.

V. SKELETON COUPLING

While neighborhood coupling has the advantage of incorporating the topology of the current state of the network into the coupling between layers, this approach does not directly address our desire to improve community carryover between layers, as the neighborhood of a node is distinct from its community assignment within that layer. We therefore propose a novel method of non-diagonal coupling that we call *skeleton coupling* that is designed to link network layers based on the static community structure within layers, therefore promoting the correct temporal carryover of community labels.

The main idea of skeleton coupling is to assign interlayer links to a node either sparsely or densely depending on its temporal neighborhood history creating temporal channels between snapshots. Moreover, by definition of a dynamic community, interlayer coupling links should only exist between the temporally carried over communities because these links are directional maps (due to the asymmetric nature of time), mapping a previous state of the system into a future state. We therefore start by finding the static communities in every snapshot (network layer) in order to determine the domain and range of these maps. This step could be performed using any static community detection method, although here we use the same static version of the DCD algorithm applied later (Fig.4B).

Once all of the static community partitions have been determined for a temporal network T , for a snapshot G_t , we can write $P_t = \{C_1, C_2, \dots, C_p\}$ for all t , where C_i consists of nodes, σ_α^t , of the network belonging to the community C_i . We can then define the k -skeleton of each community in P_t in the static layer G_t as a simplicial complex $\{SC^k\}_{C_i}^t$. For now, we will focus on the case $k \leq 1$ for computational simplicity. Each 1-skeleton describes the nodes of the community and the unweighted

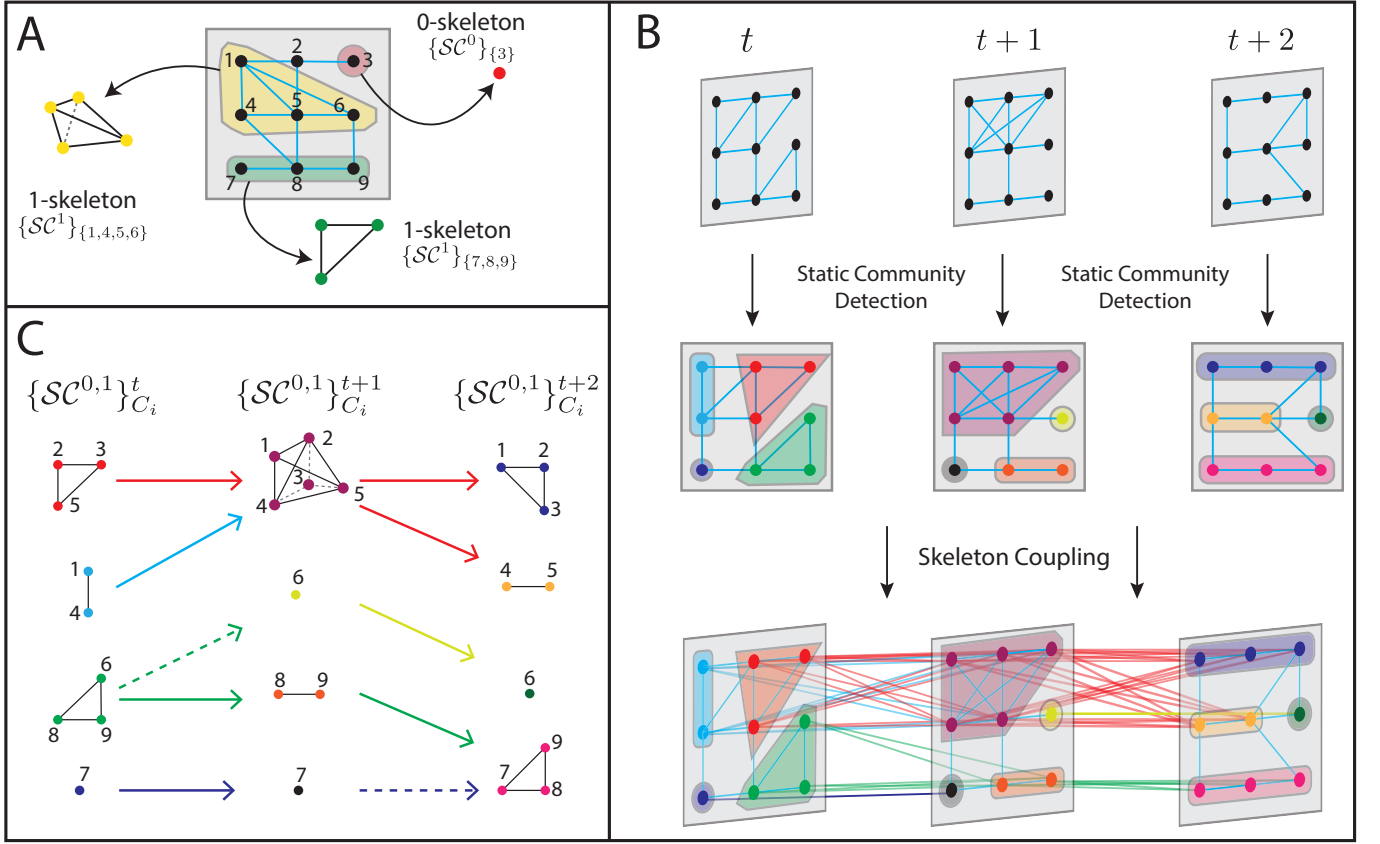


FIG. 4. **Skeleton coupling.** **A.** Skeletons of given sets (denoted by color) with different numbers of nodes. If the set has size larger than 1, we utilize the associated 1-skeleton whereas if the sets have size equal to 1, they can only have 0-skeletons. **B.** Schematic of our proposed skeleton coupling framework for determining non-empirical interlayer edges in dynamic community detection. Static community detection is performed on individual layers to find the communities in each layer (indicated by colors). Interlayer edges are then assigned via skeleton coupling, and dynamic community detection is applied to the resulting temporal network. **C.** The set matching algorithm performed by skeleton coupling on a toy network. From left to right, each column represents the skeletons of the communities within the static layers G_t , G_{t+1} and G_{t+2} shown in B. Solid arrows indicate interlayer edge assignments, whereas dashed arrows indicate no interlayer coupling. Colors of the arrows indicate the community label to be carried over to the next snapshot. In order to determine the interlayer edges between layers G_t and G_{t+1} , we compare the skeletons that vertices constitute. See the text for descriptions of interlayer edges between layers.

edges (1-simplex) fully-connecting them, i.e., $\{SC^1\}_{C_i}^t = \{(\sigma_\alpha^t, \sigma_\beta^t) | \sigma_\alpha^t, \sigma_\beta^t \in C_i\}$. Thus, a skeleton of the community C_i of size k is the k -clique consisting of the nodes whose community label, belonging to C_i , will be temporally carried over (or not) to the next snapshot (Fig. 4A). One important observation here is that singleton communities can only have a 0-skeleton, $\{SC^0\}_{C_{i_0}}^t = \{\sigma_\alpha^t | \sigma_\alpha^t \in C_{i_0}\}$, since $|C_{i_0}| = 1$ and a 1-clique is nothing but a vertex with no edges.

For any node σ_α^t in layer G_t , there are then two possibilities: 1) σ_α^t can belong to a community of size greater than or equal to 2 ($|C_\alpha| \geq 2$ and σ_α^t is part of a 1-skeleton $\{SC^1\}_{C_\alpha}^t$), or 2) it can be a singleton community ($|C_\alpha| = 1$ and σ_α^t has a 0-skeleton $\{SC^0\}_{C_\alpha}^t$). Next, we look at σ_α^t 's counterpart in the layer G_{t+1} to see if σ_α^{t+1} is part of a 0 or 1-skeleton. In order to determine how to design the interlayer coupling, we then consider all 4 possibilities of combinations between the skeletons of σ_α^t and σ_α^{t+1} :

case i: σ_α^t and σ_α^{t+1} are both 0-skeletons: We assign an undirected interlayer edge $(\sigma_\alpha^t, \sigma_\alpha^{t+1})$ with uniform edge weight ω (i.e. we diagonally couple 0-skeletons). This situation, in general, describes the continuation of community label that is maintained by the same singleton over time. This is seen in Fig. 4C, where σ_7^t and σ_7^{t+1} are both 0-skeletons ($\{SC^0\}_{\{7\}}^t$ and $\{SC^0\}_{\{7\}}^{t+1}$, respectively)—there is only one self-identity link $(\sigma_7^t, \sigma_7^{t+1})$ between them. Similarly, σ_6^{t+1} and σ_6^{t+2} are also linked by a single self-identity edge.

case ii: σ_α^t is a 0-skeleton and σ_α^{t+1} is part of a 1-skeleton: In this case, we do not assign any interlayer edges from σ_α^t to the next snapshot G_{t+1} since we don't want a singleton community label to persist when the singleton node joins a larger community. For example, in Fig. 4C, observe that σ_7^{t+1} is a 0-skeleton ($\{SC^0\}_{\{7\}}^{t+1}$), but σ_7^{t+2} is part of a 1-skeleton ($\{SC^1\}_{\{7,8,9\}}^{t+2}$). We therefore did not assign any interlayer links associated with this node between the two snapshots, as

indicated by the dashed arrow in the figure.

case iii: σ_α^t is part of a 1-skeleton and σ_α^{t+1} is a 0-skeleton: This case is the time-reversed version of *case ii*. We do not assign any interlayer edges from the node σ_α^t in the time step G_{t+1} since this case describes a community shrinking and splitting, and we don't want the community label of the node σ_α^t to be carried over to the next time step. Note in Fig.4C, for example, that σ_6^t is part of a 1-skeleton ($\{SC^1\}_{\{6,8,9\}}^t$) and σ_6^{t+1} is a 0-skeleton ($\{SC^0\}_{\{6\}}^{t+1}$). We therefore did not assign any interlayer links associated with this node between the two snapshots, as indicated by the dashed arrow in the figure.

case iv: σ_α^t and σ_α^{t+1} are both parts of 1-skeletons: We assign interlayer edges of uniform strength ω from every node with which σ_α^t shares a community C_{α^t} to every other node with which σ_α^{t+1} shares a community $C_{\alpha^{t+1}}$ in the snapshot G_{t+1} . Depending on the sizes of the communities that σ_α^t and σ_α^{t+1} are part of, this situation can describe multiple types of community events. Regardless, we want the community label to persist over time. In Fig.4C, notice for example, σ_3^t and σ_3^{t+1} belong to communities of size larger than 1 $C_{3^t} = \{\sigma_2^t, \sigma_3^t, \sigma_5^t\}$ and $C_{3^{t+1}} = \{\sigma_1^{t+1}, \sigma_2^{t+1}, \sigma_3^{t+1}, \sigma_4^{t+1}, \sigma_5^{t+1}\}$ (and the corresponding simplicial complexes $\{SC^1\}_{\{2,3,5\}}^t$ and $\{SC^1\}_{\{1,2,3,4,5\}}^{t+1}$, respectively). This implies we add interlayer edges from σ_3^t to $C_{3^{t+1}}$. If we look at other elements of C_{3^t} , σ_2^t & σ_5^t and their counterparts in the next layer σ_2^{t+1} & σ_5^{t+1} , we see a similar scenario, and therefore, we add links from all the nodes of the community C_{3^t} to all of the nodes of $C_{3^{t+1}}$, building a temporal bridge between them.

Skeleton coupling thus serves as a finely tuned coupling strategy based on the topological difference between singletons and larger communities in the time-varying network. Here, we use the terminology of a 'k-skeleton' from topological data analysis (TDA) references added [24–27] because we claim that the definition of a dynamic community in functional networks is in the form of k -plexes [22]. In a perfect world of noiseless data, a community of n nodes should be an n -clique, whereas in reality, a dynamic community is a set of nodes that has missing or noisy links. We therefore rely on the simplicial complex definition and usage of skeletons to account for real-world data in which true cliques are unlikely to be present within communities. We also provide a pseudo-code of the implementation of skeleton coupling in Supplementary Material 'Skeleton coupling algorithm'.

VI. APPLICATIONS OF SKELETON COUPLING TO TEMPORAL NETWORK ANALYSIS

In Section III, we showed that the MMM and Infomap algorithms were capable of detecting singleton communities within the data, but performed poorly in carrying over the correct community labels. In these previous comparisons, we focused on the effect of the resolution parameter, γ , (MMM) and the multilayer relax rate, ρ , (Infomap) as a function of the edge threshold value, T . Here, we will now fix γ and ρ and instead explore the effects of incorporating four different interlayer coupling strategies: uniform diagonal coupling, diagonal coupling with local updates, neighborhood coupling, and our newly proposed skeleton coupling. In each case, we explore the performance of the algorithm as a function of the interlayer edge weight, (T, ω) , and edge threshold value value, T . As before, we compare algorithm performance for two distinct types of community evolution scenarios: a monotonic series of community events in which an initial community expands over time until the whole network is synchronized, and a non-monotonic event in which *transient communities* appear/disappear over time.

We now show how incorporating the use of skeleton coupling into the design of networks results in improved performance of temporal carryover for both MMM and Infomap algorithms.

A. Influence of skeleton coupling with MMM

We first compare the performance of MMM under different interlayer coupling strategies. In Fig. 5(A), we present the results of using uniform diagonal coupling and diagonal coupling with local updates for an expanding community. Below the NMI plots, we show the community evolution plots of both optimal and non-optimal parameter choices. Observe that both coupling techniques yield structurally similar results, failing to identify the expanding community and instead carry over the independent community labels. This result is true for both optimal and non-optimal choices of coupling parameters.

Next, we study non-diagonal coupling approaches using neighborhood coupling and skeleton coupling. Notice that both of these non-diagonal approaches succeed in detecting the expanding planted dynamic community. However, neighborhood coupling fails to temporally carry over the singleton communities, assigning a different community label to each node at every layer, resulting in a total of 235 communities. On the other hand, skeleton coupling correctly carries over the singleton communities and results in a total number of detected communities that is within reasonable range of the ground truth. We also see an overall improvement in the performance of the algorithm for non-optimal parameter regions: parameter regions that are near optimal (yellow boxes) can partially recover the expanding community correctly.

In Fig. 5(B), we next examine the performance of different coupling strategies in correctly detecting transient communities in the data. Notice that both diagonal coupling strategies perform relatively well in finding planted *transient communities* within a

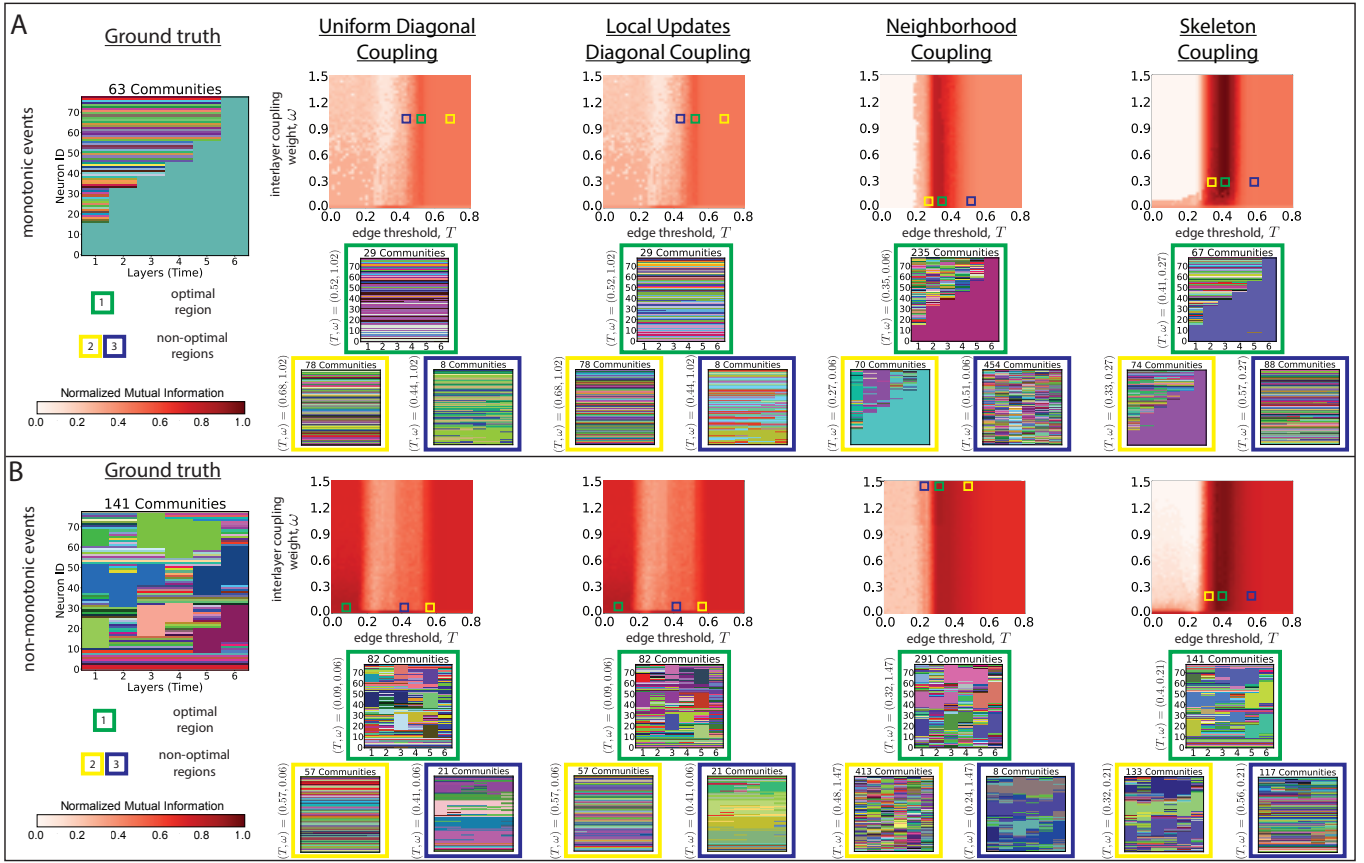


FIG. 5. **Comparison of different interlayer coupling strategies for MMM.** Comparison of different interlayer coupling heuristics for $N = 78$ neurons undergoing **A.** expanding community events with 63 total community labels and **B.** transient community events with a total of 141 community labels. Community labels are depicted by color. Parameter landscapes show algorithm performance measured by the NMI in the (T, ω) parameter space. The configuration model was chosen as the null model and the resolution parameter was equal to 0.94 for the expanding events in A and 1.46 for transient events in B. Under each parameter space, we illustrate *example partitions* found by the MMM algorithm within the bounds of optimal and non-optimal regions highlighted by green, yellow and blue rectangles, in the order of descending NMI, respectively.

layer. However, while some singleton community labels are correctly temporally carried between layers, the diagonal coupling strategies perform poorly in correctly carrying over the transient community labels between snapshots.

When using non-diagonal coupling strategies, we observe that by both neighborhood coupling and skeleton coupling perform well in correctly detecting and carrying over transient community labels. However, neighborhood coupling performs poorly at correctly carrying over independent community labels which results in a high number of total detected communities. Skeleton coupling results in not only correctly detecting and carrying over transient communities, but is also able to correctly carry over independent community labels, resulting in higher performance values. Overall, skeleton coupling outperforms the other coupling heuristics when combined with MMM for both community evolution scenarios.

B. Influence of skeleton coupling with Infomap

In Fig. 6, we show the performance of the four different coupling strategies when combined with the Infomap algorithm for the same data as in Fig. 5. Observe that in Fig. 6(A), for the expanding community, both diagonal coupling techniques seem to fail correctly detecting the neurons contained in the first a few snapshots of the temporal network as part of the expanding community, possibly due to the number of snapshots in the temporal network. However, these coupling schemes perform fairly well at capturing the temporal carry over of singleton community labels.

For the case of the non-diagonal coupling schemes, both non-diagonal approaches correctly identify the expanding community. However, neighborhood coupling fails to temporally carry over the singleton communities, assigning each node a different community label in every layer. In contrast, skeleton coupling correctly detects the temporal carryover of singleton communities,

resulting in a relatively good match between the detected evolution of communities and the ground truth.

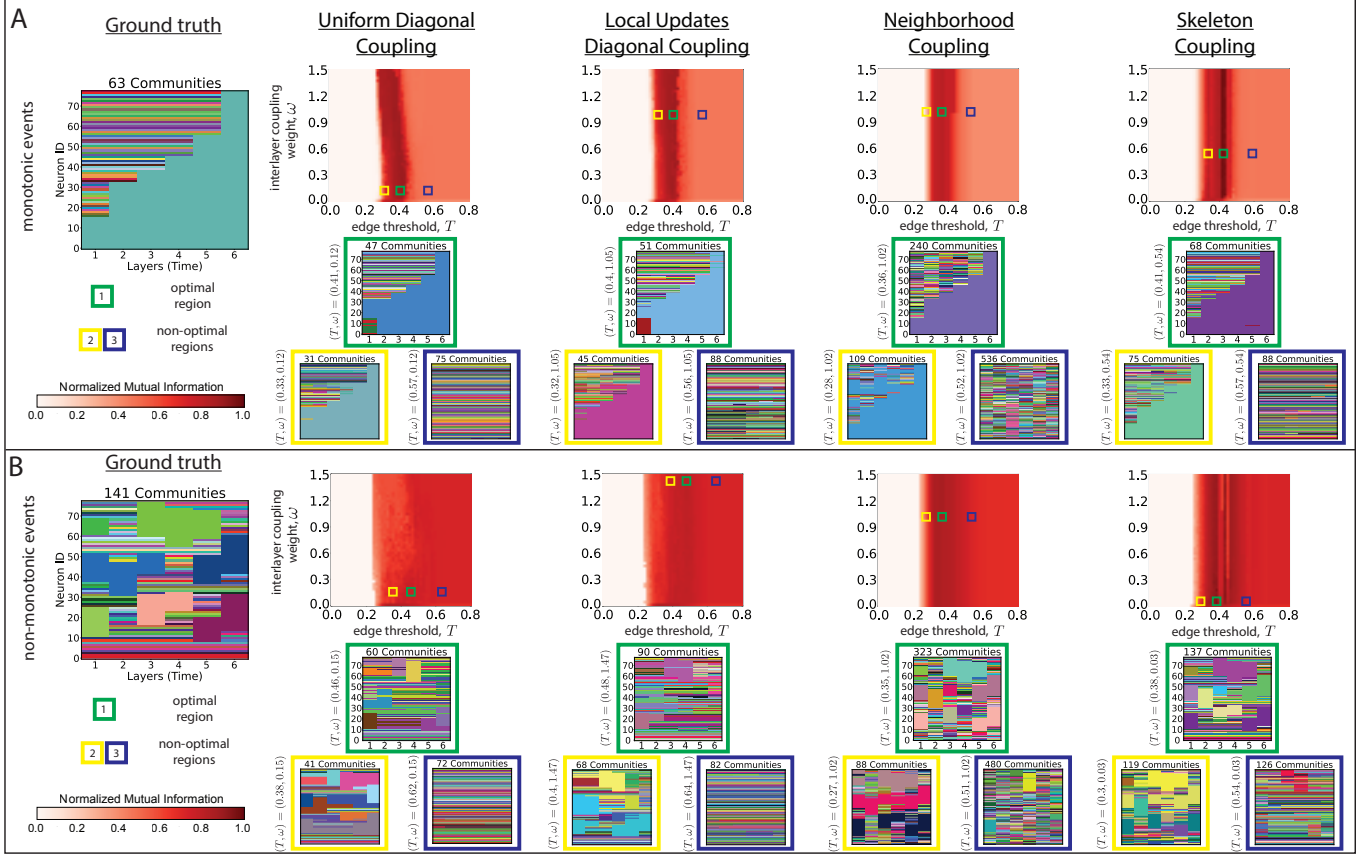


FIG. 6. **Comparisons of different interlayer coupling strategies for Infomap.** Comparison of different interlayer coupling heuristics for $N = 78$ neurons undergoing **A.** expanding community events with 63 total community labels and **B.** transient community events with a total of 141 community labels. Community labels are depicted by color. Parameter landscapes show algorithm performance measured by the NMI in the (T, ω) parameter space. The multilayer relax rate was set to 0.2 in both panels. Under each parameter space, we illustrate *example partitions* found by the MMM algorithm within the bounds of optimal and non-optimal regions highlighted by green, yellow and blue rectangles, in the order of descending NMI, respectively.

In Fig. 6(B), we explore the performance of the coupling strategies to detect transient communities in the data. Interestingly, when combined with the Infomap algorithm, diagonal coupling approaches perform very poorly, failing to identify the communities in each layer. Further, the use of these coupling strategies results in a tendency for the community labels of all nodes, regardless of whether they belong to a singleton or a larger community to be carried over. On the other hand, we again find that non-diagonal coupling approaches perform better than diagonal coupling, as indicated by the NMI values (darker shade of red). Indeed, example partitions show that both neighborhood coupling and skeleton coupling correctly identify the planted *transient communities*. However, neighborhood coupling fails to temporally carry over singletons (similar to Fig. 6(A)), increasing the total community labels. Similarly, skeleton coupling correctly performs temporal carry overs of singleton communities and shows a high correlation between the detected community evolution and ground truth.

VII. DISCUSSION

Real-world complex systems exhibit dynamical behavior in which the state of the system changes over time. Subsequently, temporal networks and dynamic community detection (DCD) can be used to assess the evolution of network communities. Here, we examined 5 different DCD algorithms and showed that current methods for these algorithms fail in data with many singleton communities and transient events. We also found that algorithms that employed interlayer edge coupling strategies (MMM and Infomap) performed better at identifying singleton communities. Further, the use of non-diagonal coupling strategies additionally resulted in superior temporal carryover of community assignments. We therefore developed a novel non-diagonal interlayer coupling scheme that we call *skeleton coupling*, which incorporates the temporal neighborhood history encoded in

the adjacent previous network states in order to algorithmically determine the placement of interlayer edges. Skeleton coupling outperformed existing interlayer coupling schemes by correctly temporally carrying over both singleton and large community labels in synthetically generated data.

Skeleton coupling builds upon the idea that singleton communities are topologically different than larger size communities. We think of dynamic communities as 1-skeletons (or cliques of partitions) independent of their connectivity in the network. In other words, given a partition of a network into communities, the 1-skeleton of a community is the fully connected subnetwork nodes which doesn't have any other outside connections, discretizing the communities from the rest of the network. Since a singleton community i.e., a 0-skeleton, does not have any edges within, it cannot have a 1-skeleton, whereas a larger size community containing edges between the members of the community can have at least 1-skeleton. Therefore, a 0- and 1-skeleton are topologically different, and they have to be coupled differently. By considering the time evolution of skeletons of communities on a temporal network, skeleton coupling algorithmically links connected components of temporal networks, which corresponds to assigning interlayer edges in the discretized versions of communities in the skeleton representation.

The development of novel non-diagonal coupling schemes is also motivated by the fact that when diagonal coupling schemes are used, the importance of selecting the proper edge weight, threshold, and DCD algorithm can be additionally complicated. In our parameter space plots of Figs. 5 and 6, we can make a general observation that the value of the interlayer edge weight seems less important than the value of threshold parameter, as seen by the similar color value of the NMI that extends vertically throughout the plots. In fact, when comparing Figs. 5A and B using the MMM algorithm, it is clear that the optimal threshold parameter is highly dependent on the type of community event for the diagonal coupling schemes. This effect is much less pronounced for the non-diagonal coupling schemes. We again see a similar effect when looking at the performance of Infomap in Fig. 6. Here, for diagonal coupling schemes, we again see differences in the regions of optimal parameters between panels A and B. Interestingly, there is also more dependence on the choice of edge weight for diagonal coupling schemes used with Infomap. Further, when employing non-diagonal coupling schemes (neighborhood and skeleton), the optimal regions in Figs. 5 and 6 exhibit a much stronger NMI which extends along the entire parameter space (vertically) for both expanding and transient community events, and this observation is independent of the choice of DCD algorithm. This finding suggests that non-diagonal linking schemes such as skeleton coupling can be used as a dimensionality reduction technique since the choice of optimal parameters is less dependent on the interlayer coupling edge weight, ω , type of community event, and choice of algorithm.

While non-diagonal coupling schemes show many advantages, one drawback of skeleton coupling is the computational cost of the given framework. In order to take advantage of skeleton coupling, one needs to apply static community detection to individual snapshots, as skeleton coupling utilizes the static community information in order to determine interlayer edges. This means that the static version of the DCD algorithm needs to run multiple times before running the DCD algorithm on the full temporal network, which clearly increases the computational complexity. However, on short-stacked temporal networks (low number of snapshots), the time consumption of the algorithm is not problematic given that the accuracy of the DCD algorithm is drastically improved.

Finally, we note that the same idea of skeleton coupling can be extended further to higher-order skeletons. For example, a community of size 2 is also topologically different than a community of size 3 and more, as the size 2 community can at most have a 1-skeleton, whereas the larger community can have at least a 2-skeleton which corresponds to the filled in triangles in the corresponding simplicial complex. In general, community sizes and dimensions of the associated skeletons are correlated and a community of size k can have at most a $(k - 1)$ -skeleton, which distinguishes it from larger size communities. Within our presented framework, additionally utilizing higher-order skeletons to select interlayer edges would result in the addition of subcases of the 'case iv' section of the presented algorithm. We anticipate that incorporating higher-order skeletons would improve the performance of DCD algorithms by introducing greater differences in topological coupling between layers. However, here, we only focus on skeletons up to dimension 1 due to the previously discussed computational concerns.

In summary, this work fills an important gap in the literature by comparing and contrasting various DCD algorithms and their optimal hyperparameters for performing community detection in temporal networks. In real-world data where the ground truth community structure and evolution is not known, understanding how network construction and choice of DCD algorithm affects the outcome of the detected community evolution is essential. In data sets with expected singleton and transient communities, we therefore recommend the use of non-diagonal coupling strategies such as skeleton coupling to improve algorithm performance and provide more accurate representation of community evolution.

VIII. METHODS

A. Code and Data availability

Code for the implementation of skeleton coupling can be found at [40] and an accompanying documentation for this codebase can be found at [41].

B. DCD algorithms

1. Multilayer modularity maximization (MMM)

Modularity assesses partition quality based on a comparison between the connectivity of nodes within a community and between communities, relative to what would be expected in a null model [17]. In our case, communities within layers are compared to the configuration model [42] by utilizing the Leiden solver [43] (instead of commonly used Louvain algorithm [44]). In Fig.2, We explored algorithm performance as a function of the edge threshold and resolution parameter, (T, γ) . For this analysis, all calculations were performed assuming uniform diagonal coupling with interlayer edge weight $\omega = 0.1$. For the analysis in Fig.5, we selected the optimal interlayer edge weight found from the analysis done in Fig.2 (Fig.5A, $\gamma = 0.94$; Fig.5B, $\gamma = 1.46$) and fixed this parameter in order to explore the (T, ω) parameter space for different interlayer coupling configurations.

2. Infomap

Infomap determines community structure based on the visiting times of nodes by random walkers via the map equation [18, 35]. We used the python API [19] with a directed flow model and optimized a two-level partition in order to run our analyses. We explored algorithm performance as a function of the edge threshold and multilayer relax rate, (T, ρ) . For this analysis, all calculations were performed assuming uniform diagonal coupling with interlayer edge weight $\omega = 0.1$. For the analysis in Fig.5, we selected the optimal multilayer relax rate found from the analysis done in Fig.2 (Fig.5A and B, $\rho = 0.2$) and fixed this parameter in order to explore the (T, ω) parameter space for different interlayer coupling configurations.

3. Dynamic stochastic block model (DSBM)

Stochastic block models determine community structure by trying to fit generative models to known properties of the data [20, 21]. In our experiments, we utilized *LayeredBlockState* in the graph-tool API [45] with overlapping model and edge covariates chosen as ‘real-exponential’ [20]. We ran our analyses with and without degree correction Δ (1 and 0, respectively), which we included in (T, Δ) parameter spaces as two different rows in Fig.2.

4. Dynamic plex propagation method (DPPM)

Dynamic plex propagation method is a generalization of the clique percolation method (CPM) [46]. DPPM relaxes the condition on the definitions of communities, which were n -cliques in CPM, into k -plexes on n nodes [22]. The algorithm runs on individual layers of the network to find the topologically clustered plexes used to define static communities. These community labels are then separately carried over across snapshots for mapping and matching. We used $n = k + 2$ in our analyses for $k = 2, 3$ as indicated in the rows of the (T, k) parameter space shown in Fig.2. We additionally note that one major drawback of the algorithm is its computational complexity which limited the use of this algorithm in our experiments.

5. Tensor Factorization

Tensor factorization determines community structure by approximating the bases of a vector space corresponding to the temporal network. The algorithm takes the desired number of communities, η as input, however, this quantity is usually not known in real-world data [23]. We therefore explore the (T, η) parameter spaces in Fig.2. We used a random initialization of the factorization of the tensors with 500 iterations. We averaged the first two factors (x,y-dimensions of the tensors) and multiplied it by the third dimension (time axis) of the basis elements in order to obtain community labels.

C. Synthetic Data Generation

We simulated neuronal activity of a population of $N = 78$ synthetic neurons using a homogeneous Poisson process. Similarity between firing patterns of neurons was assessed using the pairwise maximum cross-correlation between neurons, meaning that the goal of performing DCD on this data set was to detect groups of neurons with similar firing patterns. To create a temporal

network from the time-series data in our experiments, we used window-size of $\tau = 1000\text{ms}$ and $t_{max} = 6$ to create snapshots (layers) of the network.

In order to simulate monotonically growing communities, a master spike train of length $t_{max} \times \tau$ was generated with a randomly selected spike rate and jittered $\pm 5\text{ms}$ to create the master community. The size of the master community was randomly selected from different distributions (uniform, gaussian or exponential) in order to ensure robust results. Next, at every 1000ms, we generated independent spike trains of a given size (from the same distribution as the master) that synchronized their spiking activity with the master community (again by jittering the master spike train). This process lead to singleton communities joining the master community at every time window.

For non-monotonic events, we input number of communities we desired at each snapshot into our time-series generating pipeline. Within each layer, we created master spike trains that were jittered to generate the associated community. Then we ‘spaced’ these communities by generating independently firing spike trains. As a result, in each layer, we had N neurons where some were distributed into communities and some were singletons. If communities in adjacent layers intersected more than 50%, we assigned them the same dynamic community label.

After generating time series for both monotonic and non-monotonic community events, we divided the time series into windows of length $\tau = 1000$. We computed the pairwise maximum cross-correlation in each window to build snapshot representations of temporal networks that represent the underlying planted community structure. Finally, before applying any DCD algorithms, we padded the first and the last layers of every snapshot by the first and last static snapshot to avoid end point issues. Note that the community partitions in the padded layers was discarded after the algorithm was run.

D. Interlayer coupling

1. Uniform diagonal coupling

Uniform diagonal coupling was performed by adding undirected interlayer links between a node and itself in adjacent snapshots i.e. for every node $\sigma_\alpha^t \in V$ where $t \in \{1, 2, \dots, t_{max} - 1\}$, we assign an interlayer edge of constant weight ω , $(\sigma_\alpha^t, \sigma_\alpha^{t+1})$.

2. Diagonal coupling with local updates

Diagonal coupling with local updates is topologically the same heuristic as diagonal coupling, but in this case, the interlayer edge weights ω_α are allowed to vary. Given a constant edge weight ω , ω_α is equal to $\omega \cdot s$ if the change between nodal attribute at layer G_t and G_{t+1} is less than (or equal to) y standard deviations, and is equal to ω if it is greater than y standard deviations as described in [38]. We use firing rate as our nodal attribute and take $s = \frac{1}{100}$ and $y = 0.5$ in our experiments.

3. Neighborhood coupling

For neighborhood coupling, we determine a neighborhood of a node σ_α^t where $t \in \{1, 2, \dots, t_{max} - 1\}$ based on the strength of intralayer edges of σ_α^t . We sort all the neighbors of σ_α^t , N_α^t , in descending order of connection strength and take only the first $p\%$ of these neighbors $\{\sigma_\beta^{t+1}\}_{\beta \in N_\alpha^t}$ as the set of maximal neighbors which we couple with σ_α^t assigning uniform edge weights ω , where $p = 10$. We followed a similar protocol as described in [39] for normalizing the weights of outlinks and using Jensen–Shannon divergence, but we only couple nodes that are in adjacent snapshots.

E. Optimal regions

We determine the optimal regions of algorithm parameters by taking the argmax of the maximal normalized mutual information (NMI) within the parameter planes, (T, \cdot) . The corresponding *example partitions* are then shown for this parameter set. Although the same maximum value can occur at multiple (T, \cdot) pairs, we only display one example partition since different maximal example partitions generally do not differ structurally. In Figs.5 and 6, we choose the non-optimal regions by keeping the interlayer edge weight, ω , the same and varying the intralayer edge threshold, T .

F. Evaluating partition quality

We compare the performance of dynamic community detection algorithms with respect to a ground truth which we consider to be our planted community labels. Note that because different DCD algorithms use different definitions of the optimal com-

munity, we expect that different algorithms will detect different community partitions. Additionally, when applying DCD algorithms to real-world data, there is no known ground truth for comparison [47] which is why we explore synthetic data sets with different planted community evolution. Importantly, however, when exploring different interlayer coupling strategies, we are making comparisons about algorithm performance within a single DCD algorithm, meaning that we are measuring quantifiable insights about differences in algorithm performance as a function of interlayer coupling independently of the quality function used by the algorithm. We measure the similarity between true community labels U and predicted community labels V by calculating the *normalized mutual information* (NMI) [36, 37]:

$$NMI(U, V) = \frac{I(U, V)}{\max(H(U), H(V))} \quad (1)$$

where $H(\cdot)$ is the entropy and $I(\cdot, \cdot)$ is the mutual information which we choose to normalize by the maximum entropy of the labels since this approach works better with overlapping communities [48]. In addition, we illustrate the results in which we measure the quality of the partition by other metrics (ARI, NVI and Jaccard index) in Supplementary Material ‘Partition quality metrics’.

IX. ACKNOWLEDGMENT

This work was supported by the National Science Foundation (SMA-1734795 to S.F.M.).

-
- [1] Daniel M. Romero, Brendan Meeder, and Jon Kleinberg. Differences in the mechanics of information diffusion across topics: Idioms, political hashtags, and complex contagion on twitter. In *Proceedings of the 20th International Conference on World Wide Web*, page 695–704, New York, NY, USA, 2011. Association for Computing Machinery.
 - [2] A. Stopczynski, V. Sekara, P. Sapiezynski, A. Cuttone, M.M. Madsen, J.E. Larsen, and et al. Measuring large-scale social networks with high resolution. *PLoS ONE*, 9(4):e95978., 2014.
 - [3] Lijun Sun, Kay W. Axhausen, Der-Horng Lee, and Xianfeng Huang. Understanding metropolitan patterns of daily encounters. *Proceedings of the National Academy of Sciences*, 110(34):13774–13779, 2013.
 - [4] E. Valdano, C. Poletto, A. Giovannini, D. Palma, L. Savini, and V. Colizza. Predicting epidemic risk from past temporal contact data. *PLoS Computational Biology*, 11(3):e1004152., 2015.
 - [5] D. Kondor, M. Posfai, I. Csabai, and G. Vattay. Do the rich get richer? an empirical analysis of the bitcoin transaction network. *PLoS ONE*, 9(2):e86197., 2014.
 - [6] I. Scholtes, N. Wider, and R. et al. Pfitzner. Causality-driven slow-down and speed-up of diffusion in non-markovian temporal networks. *Nature Communications*, 5:5024, 2014.
 - [7] M. E. J. Newman. The structure of scientific collaboration networks. *Proceedings of the National Academy of Sciences*, 98(2):404–409, 2001.
 - [8] M. Rosvall, A. Esquivel, and A. et al. Lancichinetti. Memory in network flows and its effects on spreading dynamics and community detection. *Nature Communications*, 5:4630, 2014.
 - [9] Taylor I., Linding R., and Warde-Farley D. et al. Dynamic modularity in protein interaction networks predicts breast cancer outcome. *Nature Biotechnology*, 27:199–204, 2009.
 - [10] Rasmussen C, Dupont YL, Mosbacher JB, Trøjelsgaard K, and Olesen JM. Strong impact of temporal resolution on the structure of an ecological network. *PLoS ONE*, 8(12):e81694., 2013.
 - [11] Hae-Jeong Park and Karl Friston. Structural and functional brain networks: From connections to cognition. *Science*, 342(6158):1238411, 2013.
 - [12] D.S. Bassett, N.F. Wymbs, M.P. Rombach, M.A. Porter, and P.J. et al. Mucha. Task-based core-periphery organization of human brain dynamics. *PLoS Computational Biology*, 9(9):e1003171., 2013.
 - [13] Naoki Masuda and Renaud Lambiotte. *Guide To Temporal Networks*. Singapore: World Scientific Publishing Company, 2016.
 - [14] P. Holme. Modern temporal network theory: a colloquium. *European Physical Journal B*, 88:234, 2015.
 - [15] Rémy Cazabet and Frédéric Amblard. *Dynamic Community Detection*. Springer New York, New York, NY, 2014.
 - [16] Giulio Rossetti and Rémy Cazabet. Community discovery in dynamic networks: A survey. *ACM Comput. Surv.*, 51(2), feb 2018.
 - [17] P. J. Mucha, T. Richardson, K. Macon, M. A. Porter, and J.-P. Onnela. Community structure in time-dependent, multiscale, and multiplex networks. *Science*, 328(5980):876–8, 2010.
 - [18] Martin Rosvall and Carl T. Bergstrom. Maps of random walks on complex networks reveal community structure. *Proceedings of the National Academy of Sciences*, 105(4):1118–1123, 2008.
 - [19] Martin Rosvall. Daniel Edler, Anton Eriksson. Infomap python api. <https://mapequation.github.io/infomap/python/>.
 - [20] Tiago P. Peixoto. Inferring the mesoscale structure of layered, edge-valued, and time-varying networks. *Phys. Rev. E*, 92:042807, Oct 2015.
 - [21] Emmanuel Abbe. Community detection and stochastic block models: Recent developments. *Journal of Machine Learning Research*, 18(177):1–86, 2018.

- [22] LE. Martinet, M.A. Kramer, and W. et al. Viles. Robust dynamic community detection with applications to human brain functional networks. *Nature Communications*, 11:2785, 2020.
- [23] L. Gauvin, A. Panisson, and Cattuto C. Detecting the community structure and activity patterns of temporal networks: A non-negative tensor factorization approach. *PLOS ONE*, 9(1), 2014.
- [24] N. Otter, M.A. Porter, and U. et al. Tillmann. A roadmap for the computation of persistent homology. *EPJ Data Science*, 6(17), 2017.
- [25] Ann E. Sizemore, Jennifer E. Phillips-Cremins, Robert Ghrist, and Danielle S. Bassett. The importance of the whole: Topological data analysis for the network neuroscientist. *Network Neuroscience*, 3(3):656–673, 07 2019.
- [26] Chad Giusti, Robert Ghrist, and Danielle S Bassett. Two’s company, three (or more) is a simplex. *Journal of computational neuroscience*, 41(1):1–14, 2016.
- [27] A.E. Sizemore, C. Giusti, and A. et al. Kahn. Cliques and cavities in the human connectome. *Journal of computational neuroscience*, 44:115–145, 2018.
- [28] Clara Granell, Richard K. Darst, Alex Arenas, Santo Fortunato, and Sergio Gómez. Benchmark model to assess community structure in evolving networks. *Physical Review E*, 92:012805, Jul 2015.
- [29] Cazabet Remy, Boudebza Souâad, and Rossetti Giulio. Evaluating community detection algorithms for progressively evolving graphs. *Journal of Complex Networks*, 8, Dec 2020.
- [30] Rossetti Giulio. Rdyn, graph benchmark handling community dynamics. *Journal of Complex Networks*, 5:893–912, Dec 2017.
- [31] Marya Bazzi, Lucas G. S. Jeub, Alex Arenas, Sam D. Howison, and Mason A. Porter. A framework for the construction of generative models for mesoscale structure in multilayer networks. *Phys. Rev. Research*, 2:023100, Apr 2020.
- [32] Mel MacMahon and Diego Garlaschelli. Community detection for correlation matrices. *Phys. Rev. X*, 5:021006, Apr 2015.
- [33] Marya Bazzi, Mason A. Porter, Stacy Williams, Mark McDonald, Daniel J. Fenn, and Sam D. Howison. Community detection in temporal multilayer networks, with an application to correlation networks. *Multiscale Modeling & Simulation*, 14(1):1–41, 2016.
- [34] J. O. Garcia, A. Ashourvan, S. F. Muldoon, J. M. Vettel, and D. S. Bassett. Applications of community detection techniques to brain graphs: Algorithmic considerations and implications for neural function. *Proceedings of the IEEE. Institute of Electrical and Electronics Engineers*, 106(5):846–867, 2018.
- [35] Manlio De Domenico, Andrea Lancichinetti, Alex Arenas, and Martin Rosvall. Identifying modular flows on multilayer networks reveals highly overlapping organization in interconnected systems. *Phys. Rev. X*, 5:011027, Mar 2015.
- [36] Leon Danon, Albert Díaz-Guilera, Jordi Duch, and Alex Arenas. Comparing community structure identification. *Journal of Statistical Mechanics: Theory and Experiment*, 2005(09):P09008–P09008, sep 2005.
- [37] Marina Meilă. Comparing clusterings—an information based distance. *Journal of Multivariate Analysis*, 98(5):873–895, 2007.
- [38] Sarah F Muldoon Michael Vaiana, Ethan M Goldberg. Optimizing state change detection in functional temporal networks through dynamic community detection. *Journal of Complex Networks*, 7:529–553, Aug 2019.
- [39] Ulf Aslak, Martin Rosvall, and Sune Lehmann. Constrained information flows in temporal networks reveal intermittent communities. *Phys. Rev. E*, 97:062312, Jun 2018.
- [40] Bengier Ülgen Kılıç. Github, temporal network analysis. https://github.com/ulgenklc/temporal_network_analysis.
- [41] Bengier Ülgen Kılıç. Read the docs, temporal network analysis. <https://temporal-network-analysis.readthedocs.io/en/latest/index.html>.
- [42] Jörg Reichardt and Stefan Bornholdt. Statistical mechanics of community detection. *Phys. Rev. E*, 74:016110, Jul 2006.
- [43] V.A. Traag, L. Waltman, and N.J. van Eck. From louvain to leiden: guaranteeing well-connected communities. *Scientific Reports*, 9:5233, 2019.
- [44] V. D. Blondel, J.-L. Guillaume, R. Lambiotte, and E. Lefebvre. Fast unfolding of communities in large networks. *Journal of Statistical Mechanics: Theory and Experiment*, 10008(10):6, 2008.
- [45] Tiago P. Peixoto. graph-tool api. <https://graph-tool.skewed.de>.
- [46] G. Palla, I. Derényi, and I. et al. Farkas. Uncovering the overlapping community structure of complex networks in nature and society. *Nature*, 435:814–818, 2005.
- [47] Leto Peel, Daniel B. Larremore, and Aaron Clauset. The ground truth about metadata and community detection in networks. *Science Advances*, 3(5):e1602548, 2017.
- [48] Nguyen Xuan Vinh, Julien Epps, and James Bailey. Information theoretic measures for clusterings comparison: Variants, properties, normalization and correction for chance. *Journal of Machine Learning Research*, 11(95):2837–2854, 2010.

Supplementary Material:
Skeleton coupling: a novel interlayer mapping of community evolution in temporal networks

Bengier Ülgen Kilic^{1,*} and Sarah Feldt Muldoon^{1,2,3,†}

¹*Department of Mathematics, University at Buffalo, SUNY, New York, USA*

²*CDSE program, University at Buffalo, SUNY, New York, USA*

³*Neuroscience program, University at Buffalo, SUNY, New York, USA*

(Dated: January 27, 2023)

CONTENTS

Supplementary Note 1. Skeleton coupling algorithm	2
Supplementary Note 2. Partition quality metrics	3

* bengieru@buffalo.edu

† smuldoon@buffalo.edu

Supplementary Note 1. SKELETON COUPLING ALGORITHM

We give the pseudocode for our skeleton coupling algorithm in this section. Note that the provided algorithm is not an optimized version, but the time complexity is at most $O(N^2 \cdot t_{max})$.

Let $P_t = \{C_1^t, C_2^t, \dots, C_p^t\}$ and $P_{t+1} = \{C_1^{t+1}, C_2^{t+1}, \dots, C_r^{t+1}\}$ be the partitions for snapshots G_t and G_{t+1} , respectively, obtained by a static community detection algorithm for a node-aligned temporal network $T = \{G_1, G_2, \dots, G_{t_{max}}\}$. The interlayer links from a node σ_α^t to the nodes in snapshot G_{t+1} can be obtained by the output of ‘Algorithm 1’; the dictionary $SC[\sigma_\alpha, t]$.

Algorithm 1 Skeleton coupling

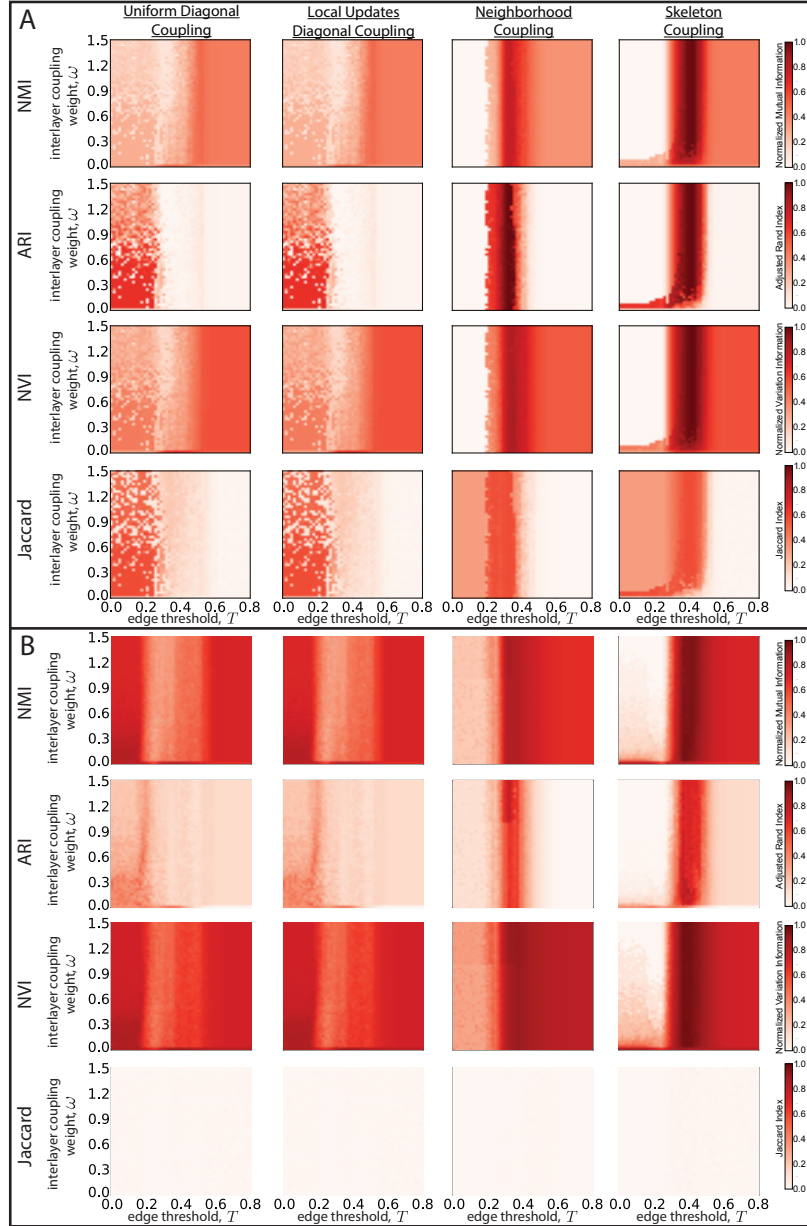
```

1: for  $t = 1$  to  $t_{max} - 1$  do
2:   for  $i = 1$  to  $p$  do
3:     for  $\sigma_\alpha$  in  $C_i^t$  do
4:       Find  $j$  such that  $\sigma_\alpha \in C_j^{t+1}$ 
5:       if  $|C_i^t| > 1$  then
6:         if  $|C_j^{t+1}| > 1$  then
7:            $SC[\sigma_\alpha, t] \leftarrow [C_j^{t+1}]$                                 {case iv}
8:         else
9:            $SC[\sigma_\alpha, t] \leftarrow []$                                 {case iii}
10:        end if
11:      else
12:        if  $|C_j^{t+1}| > 1$  then
13:           $SC[\sigma_\alpha, t] \leftarrow []$                                 {case ii}
14:        else
15:           $SC[\sigma_\alpha, t] \leftarrow [\sigma_\alpha^{t+1}]$                     {case i}
16:        end if
17:      end if
18:    end for
19:  end for
20: end for

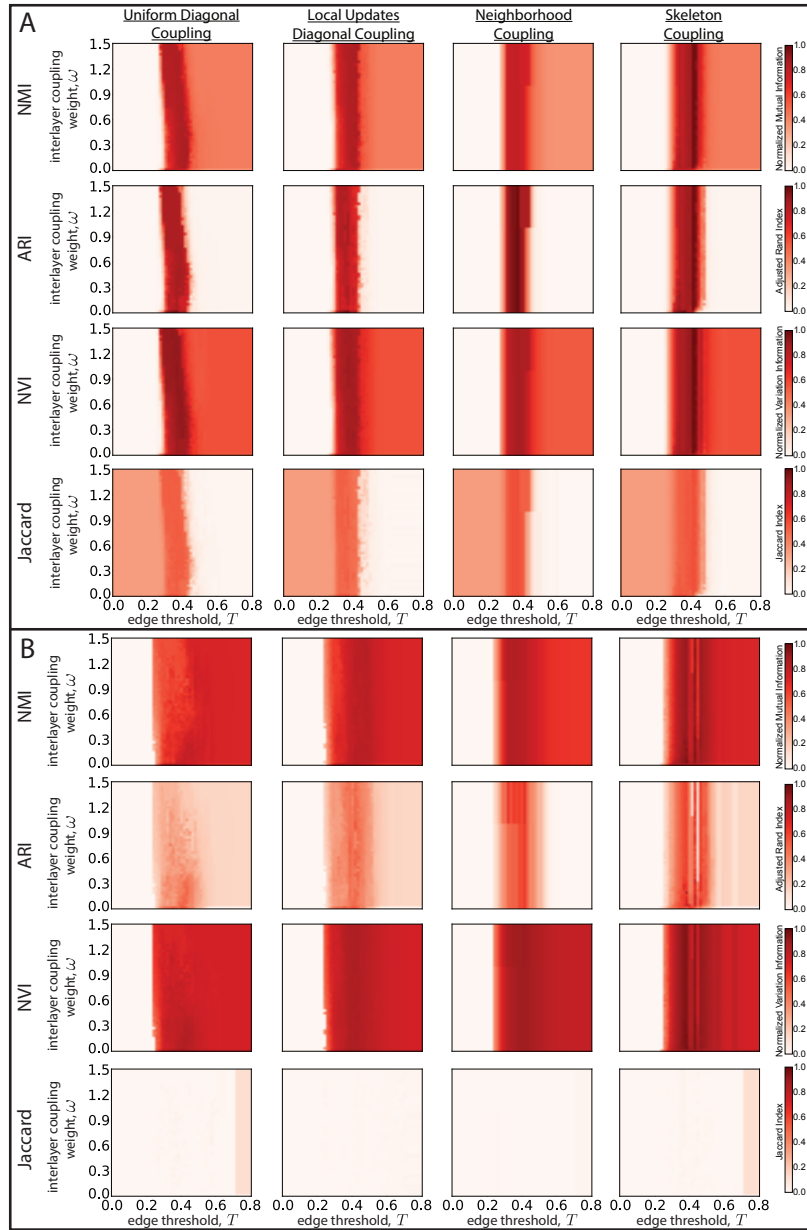
```

Supplementary Note 2. PARTITION QUALITY METRICS

In the main text, we used normalized mutual information (NMI) as our main metric to study partitions with respect to a ground truth. We test the robustness of our results for skeleton coupling by studying the parameter spaces which we examined in Figs.5 and 6 in the main text via adjusted rand index (ARI), normalized variation information (NVI) and Jaccard index in Supplementary Figs.1 and 2, respectively.



Supplementary Figure 1. **Comparisons of parameter landscapes for different information measures and interlayer coupling strategies with MMM.** We study the resulting partitions by comparing them with a ground truth as a function of NMI, ARI, NVI and Jaccard index. **A.** Monotonic events from Fig.5 in the main text. **B.** Non-monotonic events from Fig.5 in the main text.



Supplementary Figure 2. **Comparisons of parameter landscapes for different information measures and interlayer coupling strategies with Infomap.** We study the resulting partitions by comparing them with a ground truth as a function of NMI, ARI, NVI and Jaccard index. **A.** Monotonic events from Fig.6 in the main text. **B.** Non-monotonic events from Fig.6 in the main text.